THE ASTROPHYSICAL JOURNAL, 467:684–697, 1996 August 20

EVOLUTION OF MOLECULAR ABUNDANCE IN GASEOUS DISKS AROUND YOUNG STARS: DEPLETION OF CO MOLECULES

YURI AIKAWA[1]
Department of Earth and Planetary Science, University of Tokyo, Bunkyo-ku, Tokyo 113, Japan
SHOKEN M. MIYAMA
National Astronomical Observatory, Mitaka, Tokyo 181, Japan
TAKENORI NAKANO
Nobeyama Radio Observatory, National Astronomical Observatory, Nobeyama, Minamisaku, Nagano 384-13, Japan
AND
TOYOHARU UMEBAYASHI
Data Processing Center, Yamagata University, Yamagata 990, Japan
Received 1995 July 3; accepted 1996 March 26

ABSTRACT

We investigate the evolution of the molecular abundance in circumstellar disks around pre–main-sequence stars, taking into account the adsorption of molecules onto grains as well as the reactions in the gas phase. We follow the molecular evolution for some model disks, solving numerically the reaction equations. We show only the results on the abundance of CO molecules in the gas phase. There is a critical distance from the star, R_{crit}, at which the temperature is equal to the critical temperature ≈ 20 K for the adsorption of CO molecules. At $R > R_{crit}$, CO molecules are depleted rather rapidly from the gas phase mainly because of adsorption. Even in the region just inside R_{crit}, CO molecules are depleted slowly because by gas-phase reactions, they are transformed into the other molecules that can be adsorbed more easily than CO. For the minimum-mass solar nebula extended to the region of radius $R \approx 800$ AU, for example, CO molecules in the gas phase at $R > R_{crit} \approx 200$ AU are depleted by a few orders of magnitude in 10^5–10^6 yr, while at $R < R_{crit}$, the depletion of CO is not significant in these timescales. This is consistent with the recent observations of the gaseous disks around some T Tauri stars.

Subject headings: circumstellar matter — ISM: abundances — ISM: molecules — planetary systems — stars: formation — stars: pre–main-sequence

1. INTRODUCTION

Although gaseous disks containing dust were expected to exist around young stars in relation to the formation of planetary systems (see, e.g., Kusaka, Nakano, & Hayashi 1970), it took a long time to confirm their existence by observations. The first big step in the observational study of such circumstellar disks was brought about by the spectral energy distribution (SED) of T Tauri stars obtained by the *Infrared Astronomical Satellite* (*IRAS*). Many T Tauri stars have been found to have far-infrared (IR) excesses in their SEDs (Rucinski 1985; Strom et al. 1989). They were also known to have stronger blueshifted components of some forbidden lines than redshifted ones (Appenzeller, Jankovics, & Östreicher 1984). These observational facts, together with some others, strongly suggest the existence of optically thick but geometrically thin disks around T Tauri stars (Adams, Lada, & Shu 1987). The detection of radio continuum from several T Tauri stars (Beckwith et al. 1990; Ohashi et al. 1991) has confirmed the existence of at least the dust component of the disk. Because the circumstellar disk is usually optically thin to the continuum radiation at millimeter wavelengths, we can estimate the amount of dust in the disk from its intensity.

The emission lines of CO molecules have recently been detected for several T Tauri stars by radio telescopes (Skrutski et al. 1993; Guilloteau & Dutrey 1994; Handa et al. 1995). The double-peaked line profiles of CO strongly suggest the existence of rotating circumstellar disks composed of gas (and maybe dust) around these stars. Moreover, the aperture-synthesized images have been obtained for GG Tau (Kawabe et al. 1993; Dutrey, Guilloteau, & Simon 1994) and DM Tau (Saito et al. 1995). The GG Tau system is composed of two binary systems, GG Tau and GG Tau/c: GG Tau/c is located 10″ (~1500 AU in the plane of the sky) south of GG Tau. The radio image of GG Tau has a ringlike structure with an inner and outer radius of 180 and 800 AU, respectively, and one of the binary systems, GG Tau, whose components have a projected separation of about 38 AU, is located in the inner cavity. Hence, the ringlike structure must be a circumbinary disk, and the inner cavity would have been formed by the tidal disturbance of the central binary system. On the other hand, the disk around DM Tau, which is thought to be a single star, is estimated to have a radius of about 750 AU (Guilloteau & Dutrey 1994). By comparing the stellar position and the theoretical isochrones on the H-R diagram, the stellar age has been estimated to be 3×10^5 yr for GG Tau (Beckwith et al. 1990) and 1×10^6 yr for DM Tau (Handa et al. 1995). The antenna temperatures of the ^{12}CO, ^{13}CO, and $C^{18}O$ lines of these disks are widely different from each

[1] Present address: National Astronomical Observatory, Mitaka, Tokyo 181, Japan.

other. This suggests that the disks are not fully optically thick at least for the ^{13}CO and $C^{18}O$ lines. Therefore, we can estimate the amount of CO molecules in these disks from their intensities.

The mass of the disk, M_D, can be estimated from the intensities of the CO lines by assuming the CO abundance in the gas phase and also from the intensity of the dust continuum by assuming the dust/gas abundance ratio. The mass of the disk around a T Tauri star is an important parameter because it must determine the masses of the planets to be formed, and even the formation process of the planets may depend on it (see, e.g., Cameron 1985; Hayashi, Nakazawa, & Nakagawa 1985). However, if the abundances of CO and dust in the disks are the same as those estimated by the observations of molecular clouds, the disk mass estimated from the CO emission lines, $M_{D(CO)}$, is over 10 times lower than the disk mass estimated from the dust continuum, $M_{D(dust)}$, both for GG Tau and DM Tau, as described below.

The ringlike images of GG Tau have been obtained both from the CO emission-line observation and from the 2.6 mm radio continuum observation with the IRAM interferometer (Dutrey et al. 1994). Resemblances between the two images strongly suggests that the same part of the disk has been observed, and therefore it is meaningful to compare $M_{D(dust)}$ with $M_{D(CO)}$. Simon & Guilloteau (1992) obtained $M_{D(dust)} \approx 0.13\ M_\odot$ from the data of the radio continuum observation by adopting the mass absorption coefficient $\kappa_\nu(2.6\ mm) = 0.01\ cm^2\ g^{-1}$, following Beckwith et al. (1990), which is larger than that for the interstellar dust by an order of magnitude. On the other hand, Dutrey et al. (1994) obtained $M_{D(CO)} \approx 1.3 \times 10^{-3}\ M_\odot$ from the data of the ^{13}CO line observation by adopting the normal abundance ratio of ^{13}CO. The $C^{18}O$ emission line has not been detected: assuming the abundance ratio $C^{18}O/H_2 = 1.4 \times 10^{-7}$, the upper limit to the disk mass, $M_{D(CO)}$, is estimated to be $1.5 \times 10^{-3}\ M_\odot$. This upper limit should be more important than the mass estimated from the ^{13}CO line because the $C^{18}O$ line is more transparent in the disk. Dutrey et al. (1994) conclude that $M_{D(CO)}$ is more than 20–100 times lower than $M_{D(dust)}$ for the disk around GG Tau if the molecular abundances are the same as in the molecular clouds. Similarly, Guilloteau & Dutrey (1994) obtained $M_{D(CO)} \sim 0.05 M_{D(dust)}$ for the disk around DM Tau. However, in the case of DM Tau, there is a possibility that the dust continuum is emitted mainly from the inner region of the disk where the CO emission lines are optically thick because the inner cavity of the disk around DM Tau must be very small, if even present.

One may attribute this discrepancy in the disk masses to the selective loss of the gas component from the disks. However, the solid particles in the disks must be very small; otherwise, the thermal emissivity is too low to explain the observed continuum intensities. Therefore, the coupling between dust and gas is so tight that it is difficult to remove selectively the gas from the disk. A reasonable explanation of the discrepancy in the disk masses would be that CO is depleted from the gas phase in the disks or that the ratio CO/H_2 in the disks is much lower than that in molecular clouds.

To see whether or not the CO depletion can explain the discrepancy in the disk masses, we have to investigate the abundance of various molecules in the physical conditions appropriate for the circumstellar disks, where the density and the temperature are significantly higher than those in molecular clouds. Moreover, the stellar ages of GG Tau and DM Tau seem to be significantly different from each other. Therefore, it is desirable to investigate the time dependence of the molecular abundances in circumstellar disks.

In this paper, we shall investigate the evolution of the molecular abundance under physical conditions appropriate to the circumstellar disks by solving the chemical reaction equations and obtain the distribution of the abundance of various molecules in the disk at various evolutionary stages. In this way, we may be able to find out whether the chemical reactions can resolve the discrepancy in the disk masses. Moreover, because the molecular abundance in the circumstellar disks may be quite different from that in molecular clouds as suggested by the observations cited above, comparison with theoretical study on the abundance of various molecules must be inevitable to extract meaningful results from observations.

Although much work has been done on the molecular abundance in molecular clouds (see, e.g., van Dishoeck et al. 1993 and references therein; Bergin, Langer, & Goldsmith 1995), the density of molecular clouds is so low ($\sim 10^4$ H_2 molecules cm^{-3}) that these results would not be applicable to the circumstellar disks ($\sim 10^9$ H_2 molecules cm^{-3} at the radius of 100 AU; see § 2). Although some works have been done on the molecular abundance in the circumstellar disks, they are restricted to the region within a few AU from the central star, which is too small to be resolved with the present-day radio telescopes (Prinn 1993; van Dishoeck et al. 1993, and references therein). The present work will be the first one that can be compared with the recent millimeter-wave observations of the disks around T Tauri stars.

In § 2, we describe the chemical reaction network and the model of the circumstellar disk. In § 3, we show the numerical results on the evolution of the molecular abundance and the distribution of CO molecules in the disks at some evolutionary stages. In § 4, we compare our results with the observational results obtained at radio wavelengths. In § 5, we discuss the influence of some processes on the molecular abundance, which are neglected for simplicity in the previous sections, such as photodissociation of molecules, nonthermal desorption, mixing of matter, and coalescence and sedimentation of dust grains in the disk.

2. THE MODEL

2.1. *The Disk Model*

As a typical model of the circumstellar disk, we adopt the so-called minimum-mass solar nebula (Hayashi 1981) extended to the outer radius of about 10^3 AU. In this model the surface density Σ of the disk is given by

$$\Sigma(R) = 1.7\left(\frac{R}{100\ \mathrm{AU}}\right)^{-3/2}\ \mathrm{g\ cm^{-2}}, \qquad (1)$$

where R is the distance from the central star; we adopt the cylindrical coordinates (R, Φ, Z) with the equatorial plane of the nebula at the $Z = 0$ plane. Equation (1) has been obtained by redistributing smoothly the matter of the present solar system restored to the solar abundance. Although the total mass of the disk would be very large if equation (1) holds up to very large R, we presume that there must be a cutoff on $\Sigma(R)$ at some radius, e.g., $R \approx 800$ AU.

The temperature distribution in the disk is complicated. In this paper, we adopt the distribution used by Hayashi (1981),

$$T(R) = 28\left(\frac{R}{100\ \mathrm{AU}}\right)^{-1/2}\left(\frac{L_*}{1\ L_\odot}\right)^{1/4}\ \mathrm{K}\,, \qquad (2)$$

where L_* is the luminosity of the central star. We take $L_* = 1\ L_\odot$ and assume that the disk is isothermal in the Z-direction. Equation (2) may be obtained by equating the absorption rate of the radiation from the central star with the emission rate of the thermal radiation, and to be exact, it may hold only at the surface region (large $|Z|$) that is exposed to the stellar radiation. However, because the dust in the surface region emits thermal radiation at much longer wavelengths than the stellar radiation, where the opacity is much lower, the energy is transported inward by the radiation. Therefore, the disk may be nearly isothermal in the Z-direction (Kenyon & Hartmann 1987).

Another possible temperature distribution may be that obtained by Kusaka et al. (1970), which is given by

$$T(R) = 14\left(\frac{R}{100\ \mathrm{AU}}\right)^{-3/7}\left(\frac{L_*}{1\ L_\odot}\right)^{2/7}\left(\frac{M_*}{1\ M_\odot}\right)^{-1/7}\ \mathrm{K}\,, \qquad (3)$$

where M_* is the mass of the central star. This has been obtained by solving the hydrostatic equilibrium of the disk in the Z-direction and the energy balance at the surface layers of the disk. Because such a disk has a relative thickness increasing with R, it is now called a "flared" disk (Kenyon & Hartmann 1987). The differences in the R- and L_*-dependence between equations (2) and (3) are very small, though the value of the temperature is different by a factor of ~ 2 in the region $R \approx 100$–800 AU in which we are interested. In deriving equation (3), we assume that the disk is sufficiently opaque to the thermal radiation. However, with the mass distribution given by equation (1), we have $\Sigma < 2$ g cm^{-2} at $R \gtrsim 100$ AU, while the opacity at $T < 30$ K is smaller than 0.15 cm^2 g^{-1} (Pollack, McKay, & Christofferson 1985). This means that the disk is transparent to the thermal radiation at least at $R \gtrsim 100$ AU. Because the emissivity of thermal radiation of a transparent disk per unit area is lower than that of an opaque disk if the temperature is the same, the temperature must be higher than equation (3) at $R \gtrsim 100$ AU. Thus, equation (2) may be a better approximation. We shall discuss in § 3 how the distribution of CO in the gas phase is affected by the temperature distribution.

From the hydrostatic equilibrium in the Z-direction with the mass distribution given by equation (1) and the temperature distribution given by equation (2), the density distribution by the number of hydrogen nuclei is given by

$$n_{\mathrm{H}}(R, Z) = 2.0 \times 10^9\left(\frac{R}{100\ \mathrm{AU}}\right)^{-11/4} \times \exp\left(-\frac{GM_*\,\mu m_{\mathrm{H}}}{RkT}\right)\exp\left[\frac{GM_*\,\mu m_{\mathrm{H}}}{kT(R^2+Z^2)^{1/2}}\right]\mathrm{cm}^{-3}\,, \qquad (4)$$

where G is the gravitational constant, μ is the mean molecular weight of the gas, m_{H} is the mass of a hydrogen atom, and k is the Boltzmann constant. We take $M_* = 1\ M_\odot$ and $\mu = 2.34$ in this paper.

The distribution of the temperature and the surface density in the disks around T Tauri stars have also been investigated by observations of dust continuum at infrared and millimeter wavelengths. The model of the minimum-mass solar nebula fits the results of these observations fairly well (Beckwith et al. 1990).

Radio observations have revealed that the disks around T Tauri stars have a size of several hundred AU. Because the angular resolution is not high enough at present, we will investigate only the regions outside 10^2 AU and compare the results with the observations.

2.2. *The Reaction Network*

We follow for simplicity the evolution of the molecular abundance by assuming that the density and temperature of the disk do not change with time. We will discuss the effects of the physical evolution of the disk in § 5.

Taking into account gas-phase reactions, adsorption onto grains, and thermal desorption from grains, we solve the reaction equations for many kinds of species simultaneously, which can be written as

$$\frac{dn(i)}{dt} = \sum_{j,k}\alpha_{ijk}\,n(j)n(k) + \sum_j \beta_{ij}\,n(j) - \pi a^2 n(\mathrm{grain})S\left[\frac{8kT}{\pi m(i)}\right]^{1/2} n(i) + n(i\ \mathrm{desorbable})\nu_{\mathrm{osc}}(i)\exp\left[-\frac{E_{\mathrm{ads}}(i)}{kT}\right], \qquad (5)$$

where $n(i)$ is the number density of species i in the gas phase and t is the time. The first term on the right-hand side of equation (5) represents two-body gas-phase reactions in which species i is formed by the reaction of species j and k and species $i(=j)$ is destroyed by the reaction with k. The second term represents the reactions with external particles such as the ionization by cosmic rays. We adopt the network of gas-phase reactions that is essentially the same as the one described by Prasad & Huntress (1980). We add several important gas-phase reactions and use new rate coefficients for some reactions (Duley & Williams 1984, p. 213). We can expect that this network contains all the important gas-phase reactions necessary for calculating the abundances of CO and other diatomic molecules because they are very simple molecules and most of them are well-studied species. In addition, we include the reactions on grain surfaces: formation of H_2 and recombination of ions and electrons on grain surfaces. For simplicity and clarity, we do not consider the other chemical reactions on grain surfaces because detailed mechanisms and reaction rate coefficients are not well understood.

The third term on the right-hand side of equation (5) represents the adsorption of species i onto grains, where a is the grain radius, n(grain) is the number density of grains, $m(i)$ is the mass of the gas particle i, and S is the sticking probability of a gas particle when it collides with the grain. We take $S = 0.3$–0.03 following previous work (d'Hendecourt, Allamandola, & Greenberg 1985; Hasegawa & Herbst 1993; Willacy & Williams 1993; Williams 1993 and references therein). We assume that all the grains have the same radius $a = 10^{-5}$ cm unless otherwise specified. We also assume that ions are not adsorbed on grains: this would be a good approximation because grains with positive charge are negligible compared with negatively charged and neutral grains at the density range $n_{\mathrm{H}} = 10^4$–10^{10} cm^{-3}

with which we are concerned (Umebayashi & Nakano 1990).

The last term of equation (5) represents the thermal desorption of the species i from the grain surface, where $E_{ads}(i)$ is the binding energy of the adsorbed particle i at the grain surface and $\nu_{osc}(i)$ is the oscillation frequency of particle i at the grain surface. With the harmonic oscillator approximation, the oscillation frequency is estimated as

$$\nu_{osc}(i) = \left[\frac{2n_s E_{ads}}{\pi^2 m(i)}\right]^{1/2}, \quad (6)$$

where n_s is the surface density of the adsorption sites having a value of $\sim 1.5 \times 10^{15}$ cm^{-2} (Tielens & Allamandola 1987; Herbst 1993). The adsorption energy E_{ads} depends on the species of the adsorbed particle and on the kind of grain surface. We adopt the value of $E_{ads}/k = 960$ K for the CO molecule. This value has been obtained by an experiment on the CO molecule adsorbed onto the pure CO ice substrate (Sandford & Allamandola 1988, 1990). Since CO has a much smaller dipole moment than other molecules, this value is smaller than the adsorption energies onto the substrates, which are made of the other kinds of molecules such as H_2O. There are also theoretical estimates of adsorption energies (Avgul & Kiselev 1970; Allen & Robinson 1977; Hasegawa & Herbst 1993). Hasegawa & Herbst (1993) calculated the adsorption energies of many kinds of molecules onto the carbon basal plane, and the value obtained for the CO molecule is 1.26 times higher than the experimental value cited above. Therefore, we tentatively use the values 1.26 times smaller than their theoretical values for all the atoms and molecules. Table 1 shows the adsorption energies we adopt for various atoms and molecules. Assuming that only the molecules within the lth layer from the mantle surface can effectively desorb, we determine the number density of the desorbable molecules of species i, $n(i$ desorbable), according to

$$n(i \text{ desorbable}) = n(i \text{ grain}), \quad (7)$$

when the number of the mantle layers is less than or equal to l, and

$$n(i \text{ desorbable}) = n(i \text{ grain}) \times \frac{4\pi a^2 n_s \, ln(\text{grain})}{\sum_j n(j \text{ grain})}, \quad (8)$$

otherwise, where $n(i$ grain) is the number of the adsorbed molecule i per unit volume. We take $l = 2$ in this paper. Our results are not sensitive to the value of l.

The abundances of the elements we adopt in this paper is shown in Table 2, which is the abundance in the interstellar medium in which heavy elements are depleted to some extent relative to the solar abundance forming grain cores (see, e.g., Morton 1974). We determine the initial abundance of atoms and molecules in the following way. As for molecules, we take the abundance determined by the observations of TMC-1 (Irvine, Goldsmith, & Hjalmarson 1987). The total abundance of each element obtained by adding the abundances of all the species that contain this element is usually considerably smaller than the abundance shown in Table 2. This is partly because not all the species are detected in molecular clouds and partly because there are some uncertainties in the observations. To reconcile this discrepancy, we have enhanced only the abundances of atoms. As for carbon, however, we have enhanced the abundance of CO molecules as well as that of C atoms ($\frac{3}{4}$ in the

TABLE 1

ADSORPTION ENERGIES OF ATOMS AND MOLECULES IN KELVINS

Species	Adsorption Energy
C	630
N	630
O	630
Na	9400
Mg	4200
Si	2100
S	870
Fe	3300
CH	520
C_2	960
CN	1200
CO	960
CS	1600
NH	480
N_2	960
NO	960
OH	1000
O_2	960
SiH	2300
SiC	2800
SiO	2800
SiS	3000
HS	1200
NS	1600
SO	1600
CH_2	760
NH_2	680
H_2O	1500
HCN	1400
HCO	1200
C_2H	1200
CO_2	2000
OCN	1600
H_2S	1400
OCS	2400
SO_2	2400
H_2CO	1400
NH_3	880
C_2H_2	1300
CH_3	920
CH_4	1100
HC_3N	2400
H_2CS	1800
CH_3CN	1800
CH_3OH	1600

TABLE 2

ABUNDANCES OF ELEMENTS AND GRAINS[a]

Element	Abundance
H	1.00
He	1.00(−1)[b]
C	7.86(−5)
N	2.47(−5)
O	1.80(−4)
Na	2.25(−7)
Mg	1.09(−6)
Si	9.74(−7)
S	9.14(−6)
Fe	2.74(−7)
Grain	6.24(−3)[c]

[a] The abundance is by number except for grains.

[b] $a(b)$ means $a \times 10^b$.

[c] The abundance of grain cores by mass relative to hydrogen.

TABLE 3

INITIAL ABUNDANCES OF ATOMS AND MOLECULES BY NUMBER[a]

Species	Abundance
He	1.00(−1)[b]
C	8.37(−6)
N	2.47(−5)
O	1.10(−4)
Na	2.25(−7)
Mg	1.09(−6)
Si	9.74(−7)
S	9.13(−6)
Fe	2.74(−7)
H_2	5.00(−1)
CH	1.00(−8)
C_2	2.64(−8)
CN	1.50(−8)
CO	7.00(−5)
CS	5.00(−9)
OH	1.50(−7)
SO	2.70(−9)
HCN	1.00(−8)
C_2H	4.00(−8)
OCS	1.00(−9)
H_2CO	1.00(−8)
NH_3	1.10(−8)
HC_3N	3.00(−9)
CH_3CN	5.00(−10)
CH_3OH	2.00(−9)
Electron	4.55(−9)
HCO^+	4.00(−9)
N_2H^+	2.50(−10)
HCS^+	3.00(−10)

[a] The initial abundances of the other species are set equal to zero.

[b] $a(b)$ means $a \times 10^b$.

form of CO and $\frac{1}{4}$ in the form of C) because in the dense cloud cores in which the disks will form, carbon would more likely be in the form of CO molecules than of atoms. The adopted initial abundances of atoms and molecules are shown in Table 3.

3. NUMERICAL RESULTS

In this section we investigate the evolution of the abundance of various molecules in the gas phase by solving the reaction equations numerically. First, we investigate the evolution under some fixed physical conditions in order to find out the dependence on some physical parameters such as the temperature, density, sticking probability, and grain size. Next, we investigate the evolution of the molecular abundance in some definite disk models like that described in § 2.1 and find out the distribution of CO molecules in the (R, Z) plane of the disk and also the distribution of the column density of CO at some representative epochs. In this way, we find out the distribution of the depletion factor of CO from the gas phase in the disk.

3.1. *Evolution of CO Abundance under Some Fixed Physical Conditions*

To clarify the dependence of the evolution of the CO abundance on some physical parameters, we show the numerical results for some probable ranges of the parameters.

Figure 1 shows the time variation of the abundance of CO in the gas phase relative to hydrogen for some ranges of the physical quantities: temperature T between 10 and 20 K, density n_H between 10^5 and 10^7 cm^{-3}, and the sticking probability S between 0.03 and 0.3. We have taken the grain radius $a = 10^{-5}$ cm. The thick lines in Figure 1 are for the case of $T = 15$ K, $n_H = 10^7$ cm^{-3}, and $S = 0.3$, which we call here the *standard* case. In the early stages, the CO abundance is kept nearly constant at the initial value $n(\mathrm{CO})/n_H \approx 7 \times 10^{-5}$. Soon, the adsorption proceeds, and the abundance decreases exponentially by many orders of magnitude. The bump at $t \sim 5 \times 10^4$ yr is caused by the gas-phase reaction $\mathrm{C} + \mathrm{O}_2 \rightarrow \mathrm{CO} + \mathrm{O}$: adsorption of CO is temporarily in balance with the production by this reaction. Around 10^6 yr, the abundance settles down in a quasi–steady state determined by the balance among the adsorption, desorption, and chemical reactions.

If we neglect the terms of chemical reactions in equation (5), we can obtain the evolution of the molecular abundance analytically. This solution for the standard case is shown by the dashed line in Figure 1 (*left*). For this case, this analytical solution is a good approximation to the numerical one with chemical reactions except for the bump at $t \approx (0.3\text{–}1.0) \times 10^5$ yr. For the case in which the temperature is as low as 10 K, however, the CO abundance obtained by neglecting the chemical reactions is $\sim 10^{-25}$ at $t \approx 10^6$ yr, which is 10 orders of magnitude lower than that with the chemical reactions: in this stage, the chemical reactions producing CO almost compensate the adsorption of CO.

3.1.1. *Dependence on Temperature and Density*

Figure 1 (*left*) shows the time variation of the CO abundance for some values of the temperature. The other parameters are the same as in the standard case (*thick line*). For $T \lesssim 18$ K, the abundance decreases at first exponentially with a timescale of about 10^3 yr. This is caused by the adsorption of the gas molecules onto grain surfaces. This decrease does not occur in the case of $T = 20$ K. Hence, there is a critical temperature for the adsorption. The critical temperature can be found out by comparing the adsorption rate with the desorption rate, as shown below.

Figure 2 shows the adsorption rate and the desorption rate of CO molecules per unit area of the grain surface in units of molecules cm^{-2} s^{-1}. In calculating the adsorption rate we have taken $S = 0.3$ and have used the typical CO abundance for the interstellar medium, and in calculating the desorption rate we have used equation (8). The nearly horizontal solid lines represent the adsorption rate for three values of the density n_H, and the dashed lines represent the desorption rate for three values of E_{ads}. The cross point of the solid and dashed lines gives the critical temperature T_{crit} for the given n_H and E_{ads}. This is about 19 K for $n_H = 10^7$ cm^{-3} and $E_{ads} = 960$ K. If $T < T_{crit}$, almost all CO molecules are frozen onto grain surfaces in a short time. The desorption rate is also shown for the other probable values of the adsorption energy: 1210 K is the theoretical value obtained by Allen & Robinson (1977) for the adsorption onto a carbon basal plane, and 1740 K is obtained experimentally by Sandford & Allamandola (1990) for adsorption onto the ice which is composed of H_2O and CO with the ratio $H_2O/CO = 20$ by number. Note that we use in this paper the smallest value for the adsorption energy and thus the largest value for the desorption rate among the three cases.

In the case of $T = 20$ K, the CO abundance in the gas phase decreases at $t \sim 10^7$ yr as Figure 1 (*left*) shows. This is

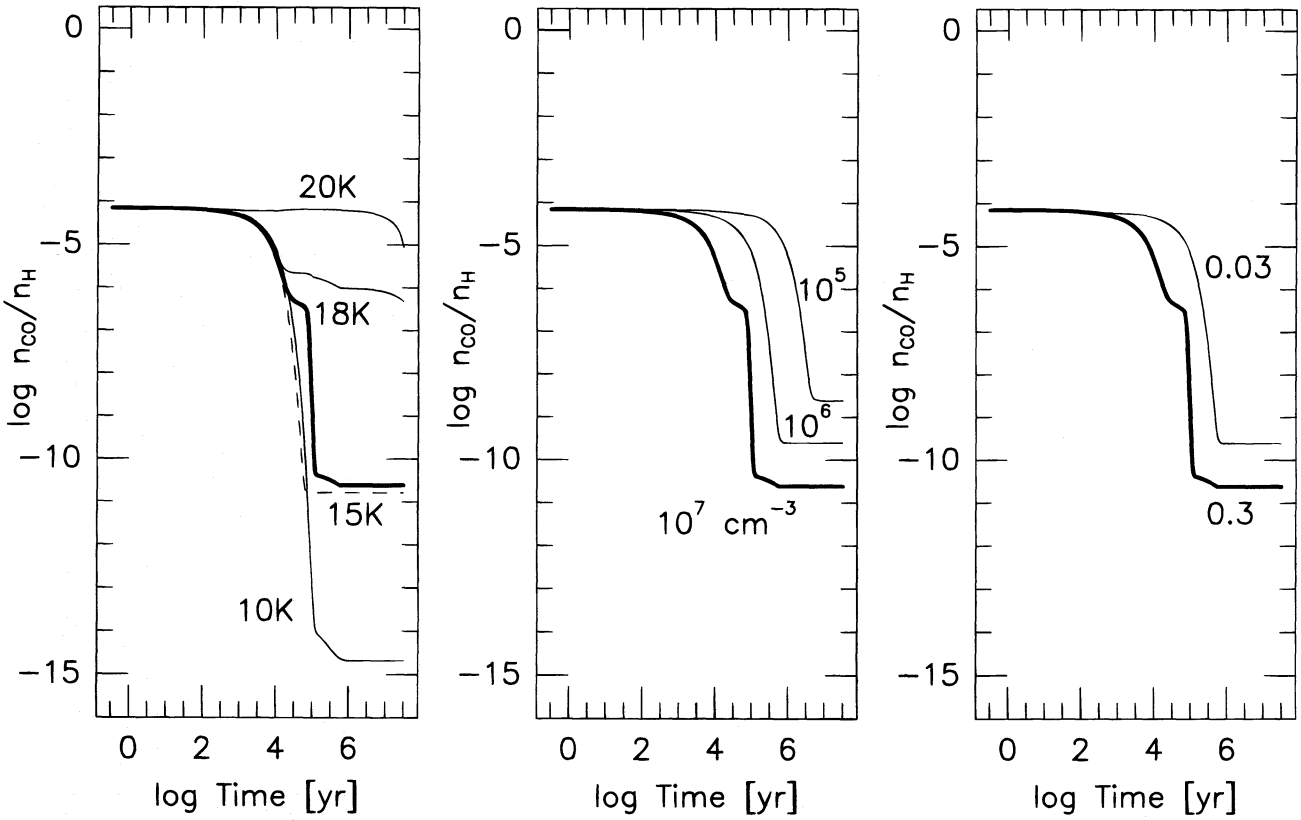

FIG. 1.—Evolution of the abundance of CO in the gas phase in various situations. *Left*: dependence on the temperature T with $n_H = 10^7$ cm^{-3} and $S = 0.3$. *Center*: dependence on the density n_H with $T = 15$ K and $S = 0.3$. *Right*: dependence on the sticking probability S with $T = 15$ K and $n_H = 10^7$ cm^{-3}. We have taken the grain radius $a = 1 \times 10^{-5}$ cm. The thick line in each panel is for the standard case in which $T = 15$ K, $n_H = 1 \times 10^7$ cm^{-3}, and $S = 0.3$. The dashed line in the left-hand panel is the case in which the gas-phase reactions are neglected with $T = 15$ K.

not due to the adsorption of CO itself. The other molecules that contain oxygen or carbon, such as H_2O and CO_2, have higher adsorption energy than CO and thus have higher critical temperature as Table 1 shows. They are adsorbed onto grain surfaces even if the temperature is 20 K. Through gas-phase reactions, CO molecules can be transformed into the other molecules that can condense more easily. In this way, the CO abundance decreases.

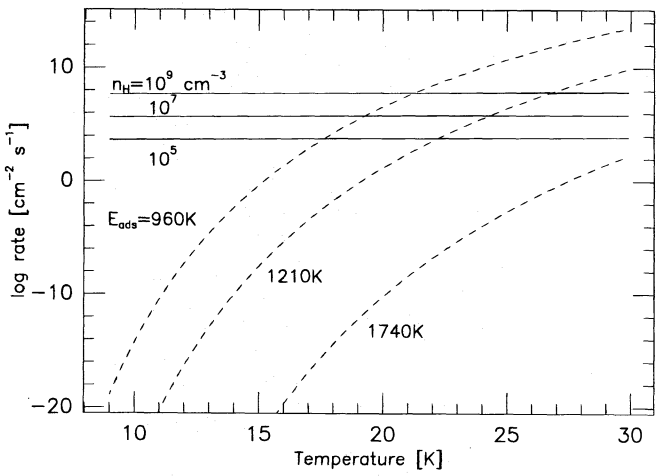

FIG. 2.—Adsorption rate and desorption rate per unit area of grain surface in units of molecules cm^{-2} s^{-1} for the sticking probability $S = 0.3$. The solid lines represent the adsorption rate for different values of n_H and are labeled with the value of n_H in units of cm^{-3}. The dashed lines show the desorption rate for different values of the adsorption energy E_{ads} and are labeled with the value of E_{ads}, which is expressed in units of kelvins conventionally. Because the adsorption rate is proportional to Sn_H, the adsorption rate for different values of S can be obtained by scaling n_H.

Figure 1 (*center*) shows the time variation of the CO abundance for some values of the density n_H. The other quantities are the same as in the standard case. We can see that the abundance decreases exponentially with a timescale that is smaller at higher density. This dependence can also be obtained by analyzing equation (5). If we neglect all the terms other than the adsorption term on the right-hand side of equation (5), we find that $n(i)$ decreases exponentially with a timescale

$$\tau_{ads} = \frac{1}{\pi a^2 n(\text{grain}) S}\left[\frac{\pi m(\text{CO})}{8kT}\right]^{1/2} = 4 \times 10^3 \left(\frac{10^7 \text{ cm}^{-3}}{n_H}\right)\left(\frac{0.3}{S}\right)\left(\frac{15 \text{ K}}{T}\right)^{1/2} \text{yr} . \quad (9)$$

Thus the adsorption time τ_{ads} is inversely proportional to the density n_H.

3.1.2. *Dependence on the Other Parameters*

In this subsection, we discuss the dependence of T_{crit} and τ_{ads}, crucial quantities for the evolution of the molecular abundance, on the other parameters, which involve significant uncertainties.

The sticking probability S of molecules onto grains is rather uncertain. Since the adsorption rate is proportional to S, the critical temperature T_{crit}, at which the adsorption rate equals the desorption rate, depends on S. However, as seen from Figure 2, even if S is smaller by an order of magnitude ($S \sim 0.03$), T_{crit} decreases by less than 1 K. Thus,

T_{crit} is rather insensitive to S. On the other hand, the timescale of adsorption, τ_{ads}, is inversely proportional to S as equation (9) shows and Figure 1 (*right*) suggests.

The adsorption rate per unit volume is proportional to the sum of the geometrical cross sections of grains in a unit volume, $\pi a^2 n$(grain), as equation (5) shows, and then the timescale of adsorption, τ_{ads}, is inversely proportional to this quantity as equation (9) shows. This quantity depends on the grain size distribution. In the above numerical calculations, we have assumed that all grains have a radius $a = 10^{-5}$ cm. If we adopt the commonly used power-law size distribution of interstellar grains

$$dn(\text{grain}) \propto a^{-3.5} da \qquad (10)$$

between the minimum radius $a_{min} = 5.0 \times 10^{-7}$ cm and the maximum radius $a_{max} = 2.5 \times 10^{-5}$ cm (Mathis, Rumpl, & Nordsieck 1977), the sum of the cross sections becomes 2.8 times larger, and then τ_{ads} becomes smaller by the same factor. However, it is to be noted that in circumstellar disks with very high density, the grain size may be different from that in the interstellar medium because of the growth by coalescence.

The adsorption energy E_{ads} is influenced by the conditions of the grain surface. The desorption rate is very sensitive and the critical temperature is rather sensitive to this parameter as Figure 2 shows. Note that the value 960 K we have adopted in this paper is for the case in which the CO molecule is adsorbed onto the pure CO ice and is lower than the values for more polar substrates like the H_2O ice.

3.2. *Distribution of CO Abundance in Circumstellar Disks*

We now investigate the distribution of gas-phase CO molecules in the circumstellar disks. First, we adopt the model of the minimum-mass solar nebula represented by equations (1), (2), and (4). By solving numerically the reaction equations (5), we follow the time variation of the abundances of various molecules at each point (R, Z) of the disk. For simplicity, we neglect the mixing of matter in the disk by accretion flow, turbulent motion, etc.: we will discuss the effects of such motions in § 5. The purpose of this section is to show how the depletion of CO proceeds in the disk and how the depletion depends on parameters such as the sticking probability and the mass of the disk.

Figures 3*a* and 3*b* show the distribution of the abundance of gas-phase CO molecules on the (R, Z) plane of the minimum-mass solar nebula at two epochs, (*a*) $t = 10^5$ yr and (*b*) 10^6 yr, for the sticking probability $S = 0.3$. The central star is at the origin ($R = 0$, $Z = 0$) outside the panel, and the horizontal axis is the midplane of the nebula. We have considered only the inside of the dashed line on which $n_H = 10^4$ cm^{-3}. The solid lines are contours of constant CO abundance and are labeled with the value of log $[n(\text{CO})/n_H]$. The abundance of CO is very low near the midplane because the timescale of adsorption, τ_{ads}, is much shorter than 10^5 yr owing to very high density. In the regions of large R and Z, τ_{ads} is long because of rather low density, and therefore CO has not yet been adsorbed much. In the region of $R \sim 500$ AU, the CO abundance is significantly higher than in the neighboring region, especially near the midplane. At the temperature of this region and at these epochs, the production of CO by the gas-phase reaction $C + O_2 \rightarrow CO + O$ counterbalances the adsorption temporarily. As the time goes on, the region of low abundance spreads as seen by comparing Figures 3*a* and 3*b*.

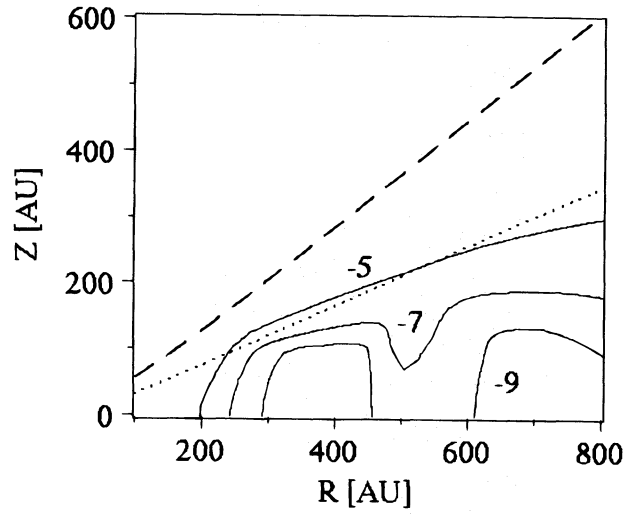

FIG. 3*a*

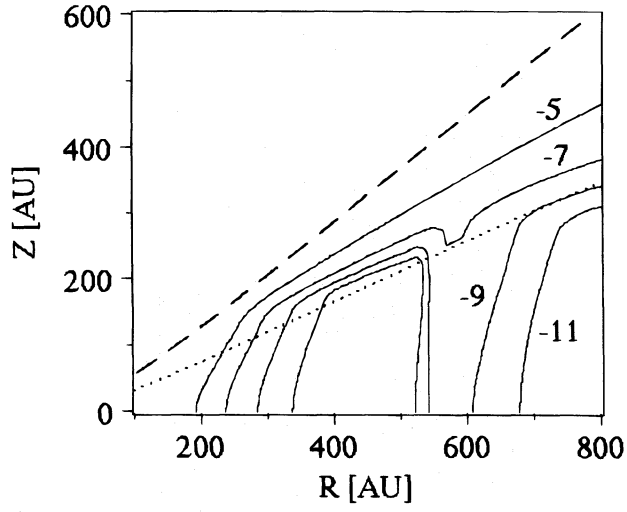

FIG. 3*b*

FIG. 3.—Distribution of the abundance of CO molecules in the gas phase on the (R, Z) plane of the minimum-mass solar nebula for the case of the sticking probability $S = 0.3$ at two epochs: (*a*) $t = 10^5$ yr and (*b*) $t = 10^6$ yr. The solid lines are contours of constant CO abundance and are labeled with a value of log $[n(\text{CO})/n_H]$. The dashed line represents the surface of the disk, which is taken at $n_H = 10^4$ cm^{-3}. The dotted line shows the layer at which the optical depth for the interstellar UV radiation is equal to unity.

Figure 4 shows the distribution of the column density of gas-phase CO molecules for the same case as in Figures 3*a* and 3*b*. The dashed line shows the column density at the initial state with the interstellar abundance $n(\text{CO})/n_H = 7 \times 10^{-5}$, and the thick solid lines show those at $t = 10^5$ and 10^6 yr. At these two epochs, the column density has a very steep slope at $R \sim 200$ AU. The temperature around 200 AU is close to the critical temperature for adsorption, T_{crit}. While the temperature in the inner region is too high for CO to be adsorbed, the outer region is cool enough for adsorption. At $R \gtrsim 300$ AU, the column density of CO increases gradually as R increases. This is because the density decreases and thus the timescale for adsorption, τ_{ads}, increases with R. By comparing the column density at two epochs 10^5 and 10^6 yr, we can confirm that the column density of CO in the gas phase decreases with time at all R. Another point to be noted is that the column density of CO decreases with time even in the region inside 200 AU, where

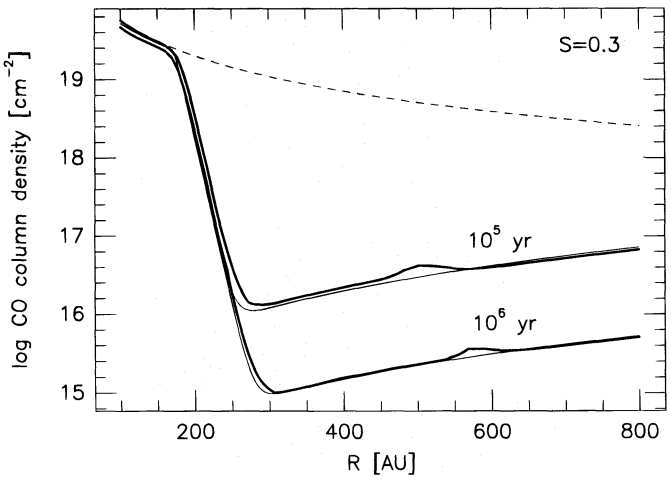

FIG. 4.—Distribution of the column density of CO molecules in the gas phase in the minimum-mass solar nebula with $S = 0.3$ at $t = 10^5$ yr and $t = 10^6$ yr (*thick solid lines*). The dashed line represents the initial column density, and thin solid lines represent the column density obtained by neglecting the gas-phase reactions.

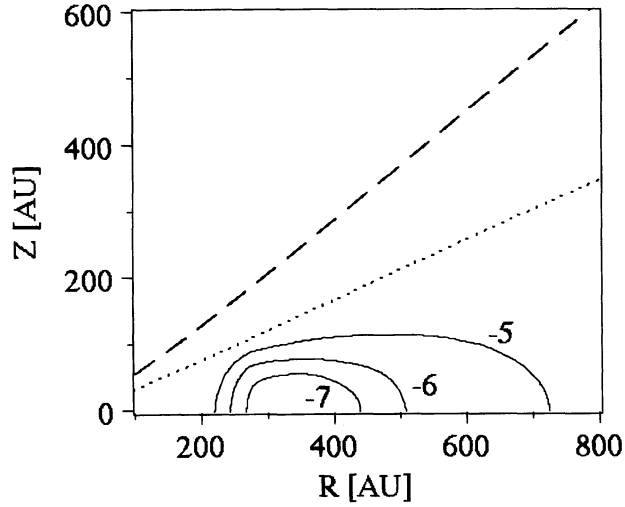

FIG. 5.—Distribution of the abundance of CO molecules in the gas phase on the (R, Z) plane of the minimum-mass solar nebula with $S = 0.03$ at $t = 10^5$ yr. The other details are the same as in Fig. 3.

the temperature is somewhat higher than the critical temperature. As discussed in § 3.1.1, the reason for this is that through gas-phase reactions CO molecules can be destroyed and transformed into other molecules, which have higher critical temperature and condense more easily than CO. The column density of CO at $R \gtrsim 200$ AU is contributed mainly by the diffuse layer of high Z at which CO is depleted by no more than 3 orders of magnitude.

The thin solid lines in Figure 4 show the column density of CO molecules that has been obtained analytically by considering only the adsorption and desorption terms in equation (5). They agree with the corresponding thick lines fairly well at $R \gtrsim 200$ AU. Thus, the gas-phase reactions are not very important in determining the column density of CO in these regions.

We define the depletion factor of CO as the ratio of the column density of CO in the initial state with the interstellar abundance $n(\mathrm{CO})/n_{\mathrm{H}} = 7 \times 10^{-5}$ to that obtained in our model. The depletion factor is obtained by comparing the dashed line with the thick solid lines in Figure 4. It amounts to a few orders of magnitude. This is because CO has been almost thoroughly depleted in the denser part of the layer and remains only in the diffuse region. At R between 250 and 800 AU, the depletion factor is 40–10^3 at $t = 10^5$ yr and 5×10^2–10^4 at $t = 10^6$ yr. The depletion factor increases with time or with the age of the disk.

We have also investigated the case of $S = 0.03$ in order to see the dependence on the sticking probability. Figure 5 shows the distribution of the CO abundance in the gas phase on the (R, Z) plane at $t = 10^5$ yr. Because the timescale for adsorption, τ_{ads}, is longer in this case, the region of low abundance is narrower. The distribution at $t = 10^6$ yr is similar to that for the case of $S = 0.3$ at $t = 10^5$ yr, which is shown in Figure 3*a*, as can be inferred from equation (9). Figure 6 compares the distribution of the column density of CO at $t = 10^5$ yr for the two cases of $S = 0.3$ and 0.03. The depletion factor at $R \approx 250$–800 AU is 2.5–100 for the case of $S = 0.03$, while it is 40–10^3 for $S = 0.3$.

To see the dependence on the disk mass, we have also investigated the disks of mass 10 and 0.1 times the mass of the minimum-mass solar nebula or, more exactly, the disks of surface density 10 and 0.1 times that of equation (1). Figures 7*a* and 7*b* show the distribution of the CO abundance on the (R, Z) plane at $t = 10^5$ yr for these disks. The adsorption of CO proceeds faster in a nebula of higher mass because of the higher density. Figure 8 shows the distribution of the CO column density for these disks. The CO column density outside 250 AU is rather insensitive to the disk mass: the difference between these models is small, and the column density for the minimum-mass solar nebula is in between. This is because the column density is determined mainly by the amount of CO molecules in the diffuse region at high Z. The denser region near the midplane, where almost all CO molecules have been adsorbed to grain surfaces, hardly contributes to the CO column density. Thus, roughly speaking, the depletion factor at $R \gtrsim 250$ AU is proportional to the disk mass.

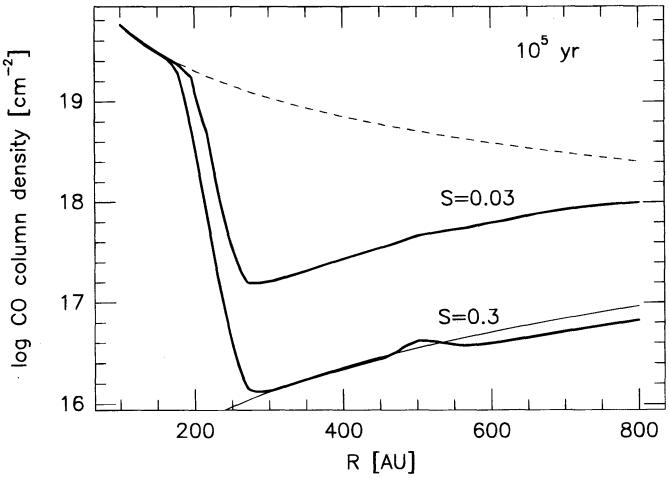

FIG. 6.—Distribution of the column density of CO molecules in the gas phase in the minimum-mass solar nebula at $t = 10^5$ yr for the two cases of $S = 0.3$ and 0.03 (*thick solid lines*). The thin solid line represents the column density at $t = 10^5$ yr with $S = 0.3$ in the case of constant temperature distribution with $T = 16$ K. The other details are the same as in Fig. 4.

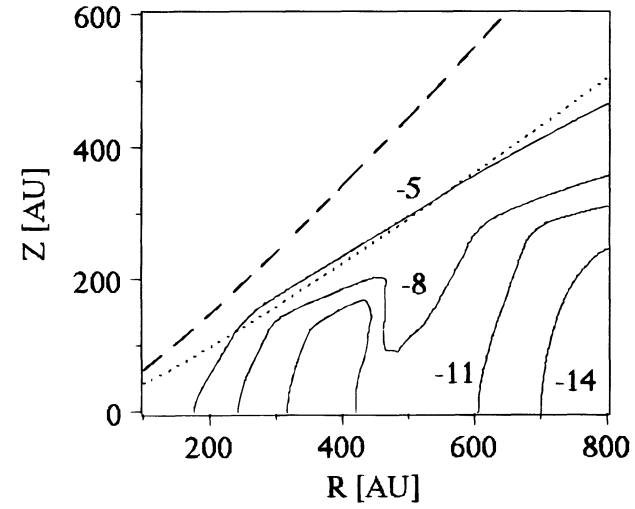

FIG. 7a

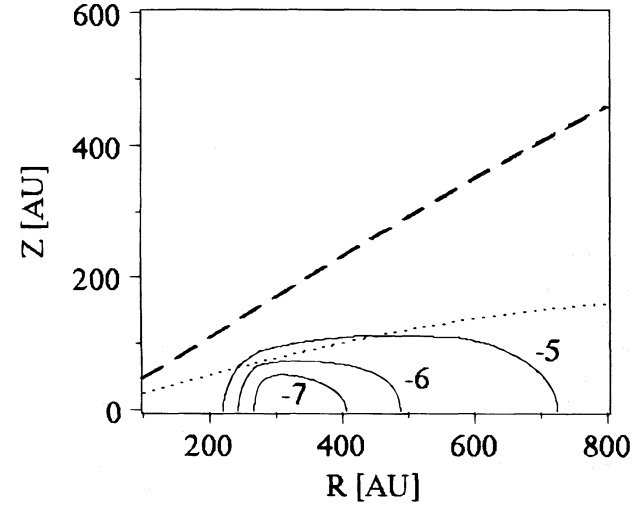

FIG. 7b

FIG. 7.—Distribution of the abundance of CO molecules in the nebula at $t = 10^5$ yr with $S = 0.3$. The disk mass is (*a*) 10 times and (*b*) 0.1 times the mass of the minimum-mass solar nebula. The other details are the same as in Fig. 3.

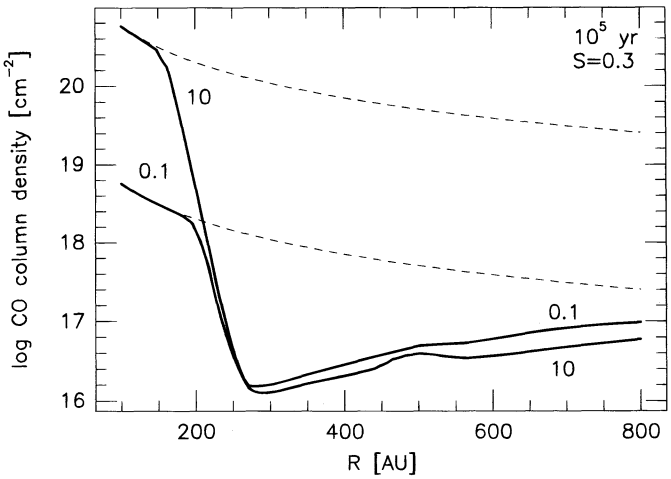

FIG. 8.—Distribution of the column density of CO molecules in the gas phase in the circumstellar disks of different masses at $t = 10^5$ yr with $S = 0.3$. Each line is labeled with the disk mass in units of the mass of the minimum-mass solar nebula. The other details are the same as in Fig. 4.

So far, we have adopted the surface density distribution of the disk, $\Sigma \propto R^{-3/2}$, as in equation (1), and the temperature distribution, $T \propto R^{-1/2}$, as in equation (2). The above result that the column density of CO is rather insensitive to the disk mass strongly suggests that the column density of CO at $R \gtrsim 250$ AU and $t \sim 10^5$ yr is insensitive to the R-dependence of Σ. To see the sensitivity of the CO depletion on the assumed temperature distribution, we have investigated the case in which the temperature is constant, $T = 16$ K, at 100 AU $\leq R \leq$ 800 AU. The result at $t = 10^5$ yr with $S = 0.3$ is shown by the thin solid line in Figure 6. The column density of CO in the region of $T < T_{\rm crit} \approx 20$ K is rather insensitive to the temperature distribution. This is because the thermal desorption of CO, whose rate is very sensitive to the temperature, is inefficient at $T < T_{\rm crit}$, and the other processes, gas-phase reactions and adsorption onto grains, are not very sensitive to the temperature. Therefore, if the temperature distribution is different, the main difference appears only in the position that separates the highly depleted region from the hardly depleted region or the position of $T = T_{\rm crit}$.

4. COMPARISON WITH OBSERVATIONS

We have investigated in § 3 the evolution of the abundance of gas-phase CO molecules for some models of the gaseous disks around young stars, taking into account the effect of the adsorption of molecules onto grain surfaces as well as the gas-phase reactions. Now we compare our results with the observational results on some T Tauri stars.

4.1. *The Depletion Factor*

We have summarized in Table 4 the depletion factor of CO molecules in the gas phase in the circumstellar disks obtained in § 3 together with that obtained by observations of some T Tauri stars. Because the disk around GG Tau has a hole of radius 180 AU and the disk around DM Tau does not seem to have such a hole, we have tabulated the depletion factor for the disk models averaged in the region $R = 100$–800 AU and in the region $R = 180$–800 AU. These depletion factors are smaller than the value averaged over $R = 250$–800 AU, which we have mentioned in the previous section, since the CO molecules inside $R = 250$ AU contribute to the total amount considerably. The masses of the disks around GG Tau and DM Tau have been estimated from the intensities of the dust continuum. The depletion factor has been estimated by comparing the disk mass estimated from the dust continuum with the mass estimated from the intensity of the CO line, assuming the interstellar abundance of CO. It should be noted that the depletion factor calculated in this way from the observational data may not give the actual depletion factor because the CO line may not be sufficiently transparent.

GG Tau is somewhat older than 10^5 yr, and the disk around it is about 2 times more massive than the minimum-mass solar nebula extended to $R \approx 800$ AU. Considering the dependence of the depletion factor on the mass and the age, we can say that our models are consistent with the observational results of GG Tau. The depletion factor at $t = 10^6$ yr averaged over $R = 100$–800 AU is ~ 5 for our models, which is significantly smaller than the value for DM Tau. The discrepancy would be worse if we consider the difference in the disk mass. However, as mentioned above, the CO abundance has been estimated from the obser-

TABLE 4

DEPLETION FACTOR OF CO IN THE CIRCUMSTELLAR DISKS OBTAINED BY OUR MODEL CALCULATIONS AND BY OBSERVATIONS

MODEL OR STAR	DISK MASS ($M_\odot$)	STICKING PROBABILITY	AGE (10^5 yr)	AVERAGED DEPLETION FACTOR	
				100–800 AU	180–800 AU
Model	0.07	0.3	1	5	30
Model	0.07	0.3	10	6	60
Model	0.7	0.3	1	7	200
Model	0.007	0.3	1	3	6
Model	0.07	0.03	1	3	6
Model	0.07	0.03	10	5	18
GG Tau	0.13	...	3	...	20–100
DM Tau.....	0.03	...	10	20	...

vations by assuming that the disk is optically thin to the CO line. For some isotopic CO ($J = 2$–1) line, the disk is transparent only when the column density of the isotopic CO molecule is less than 10^{14}–10^{15} cm^{-2} at the temperature with which we are concerned here (see also the next subsection). As seen from Figure 4, the disk is opaque to the lines of ^{13}CO and C^{18}O, not to mention ^{12}CO, at $R \lesssim 200$ AU. This would lead to an apparent depletion factor of several $\times$ 10 as in the disk of DM Tau.

4.2. *The Intensity Map*

From the distribution of CO molecules in the gas phase obtained in § 3, we can calculate the intensity map of the CO line for the disk. Hoping for comparison with observations in the future, we calculate the intensity map. For simplicity, we calculate a map for a face-on disk with the rotation axis parallel to the line of sight. Then, the intensity of the radiation I_ν at frequency ν is a function of the distance R from the central star.

We consider the radiation of frequency ν emitted by the transition of a molecule from state a to state b with transition energy $h\nu_0$. The disk is isothermal along the line of sight. If, in addition, the level population of the molecule is constant along the line of sight, the source function S_ν of the radiation at frequency ν is also constant, and we have

$$I_\nu(R) = S_\nu[1 - \exp(-\tau_\nu)] . \quad (11)$$

When the excitation temperature of the molecule is equal to the kinetic temperature of the gas, the source function S_ν is equal to the Planck function at the kinetic temperature T. The optical depth τ_ν of the disk is given by

$$\tau_\nu = \int_{\rm disk} \kappa_\nu \rho \, dZ = \int_{\rm disk} \frac{h\nu}{4\pi} n_b \left[1 - \exp\left(-\frac{h\nu}{kT}\right)\right] B_{ba} f(\nu) dZ , \quad (12)$$

where κ_ν is the opacity per unit mass at frequency ν, ρ is the density of the disk, n_b is the number density of the molecule in state b, B_{ba} is the Einstein B-coefficient, and $f(\nu)$ is a profile function. If we consider only the Doppler broadening due to the thermal motion of molecules, the line profile is given by

$$f(\nu) = \left(\frac{4\ln 2}{\pi}\right)^{1/2} \frac{1}{\delta\nu} \exp\left[-4\ln 2\left(\frac{\nu - \nu_0}{\delta\nu}\right)^2\right], \quad (13)$$

with

$$\delta\nu \equiv \nu_0 \left(4\ln 2 \frac{2kT}{mc^2}\right)^{1/2} , \quad (14)$$

where m is the mass of the molecule, and c is the velocity of light.

By means of equations (11)–(14), we calculate the intensity of the ^{13}CO ($J = 2$–1) line emitted by the minimum-mass solar nebula with $S = 0.3$ and 0.03 assuming the abundance ratio ^{12}CO/^{13}CO = 89, which is equal to the isotopic ratio ^{12}C/^{13}C in the solar system. The interstellar ^{12}C/^{13}C abundance ratio in the solar neighborhood takes a value between 50 and 100 depending on the adopted molecules (Mitchell & Maillard 1993; Hawkins, Craig, & Meyer 1993; Langer & Penzias 1993). Moreover, the chemical fractionation may decrease the ratio ^{12}CO/^{13}CO significantly. However, we adopt the above value because of various uncertainties. Figure 9 shows the distribution of the intensity at frequency ν_0 at $t = 10^6$ yr for the models with sticking probability $S = 0.3$ and 0.03. Because the disk is nearly optically thin to the ^{13}CO line at these stages in the

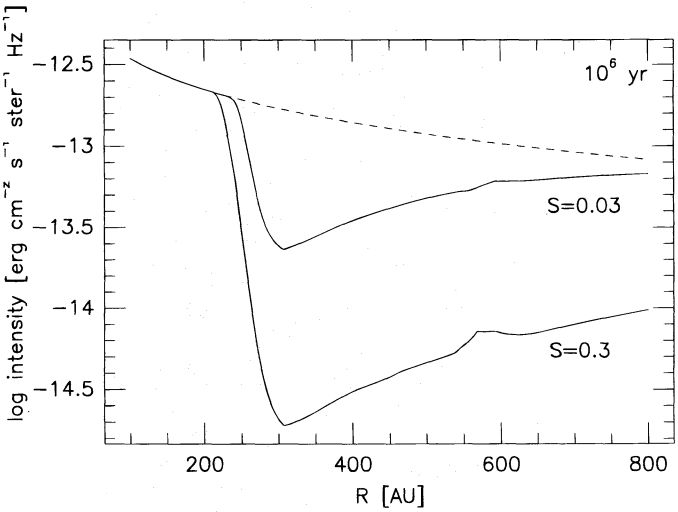

FIG. 9.—Distribution of the ^{13}CO ($J = 2$–1) emission-line intensity for the minimum-mass solar nebula with $S = 0.3$ and 0.03 at $t = 10^6$ yr (*solid lines*). The dashed line represents the initial intensity distribution.

outer region, the distribution of the intensity is similar to that of the column density. The intensity distribution for the disk around DM Tau must be similar to the distribution shown in Figure 9.

5. DISCUSSION

We have investigated the abundance of CO molecules in gaseous disks around pre–main-sequence stars, taking into account the gas-phase reactions, the adsorption of molecules onto grains, and thermal desorption from grains. We have neglected for simplicity some processes such as photodissociation of molecules by interstellar and stellar ultraviolet radiation, nonthermal desorption, mixing of matter in the disk, and sedimentation of dust grains. We discuss here the effects of these processes on the CO abundance. We also discuss the effects of the uncertainties in the disk temperature and of nonsteadiness of the disk.

5.1. *Photoprocesses*

In this subsection we investigate the effect of ultraviolet (UV) radiation on the molecular abundance in the disk. The UV radiation dissociates or ionizes molecules. Since the photodissociation rate is typically $\sim 10^{-11}$ s^{-1} for the radiation from the interstellar space, the timescale of photodissociation is $\sim 10^{11}$ s and is shorter than the age of the circumstellar disks.

The circumstellar disk is exposed to the UV radiation from interstellar space and from the central star. Although the UV radiation from the central star is 10^3–10^4 times stronger than that from interstellar space at $R \approx 100$ AU (Herbig & Goodrich 1986; Imhoff & Appenzeller 1987), it irradiates the disk obliquely and is attenuated more efficiently than the radiation from the interstellar space. The UV radiation, which can dissociate CO molecules, is attenuated not only by dust but also by CO molecules themselves: the latter is called self-shielding. The attenuation lengths by dust and by self-shielding correspond to a hydrogen column density of 5×10^{20} cm^{-2} (Duley & Williams 1984, p. 86) and a CO column density of 1.0×10^{13} cm^{-2} at the temperatures with which we are concerned here, respectively (Bally & Langer 1982). Therefore, the self-shielding is more efficient as long as the abundance of CO molecules is higher than 2×10^{-8}. However, for simplicity we consider here only the attenuation by dust. To take into account the self-shielding, we have to solve the radiative transfer and the chemical reactions simultaneously: the attenuation of the UV radiation depends on the abundance of CO molecules, and conversely the CO abundance depends on the UV flux. We leave this problem for a future work.

We make a rough estimate of the effect of photodissociation on the CO abundance in the following way. The dotted lines in Figures 3, 5, and 7 represent the layer at which the optical depth for the interstellar UV radiation due to dust is equal to unity. By assuming that all CO molecules outside this layer are destroyed by the UV radiation and that the molecular abundance inside this layer is determined by the reactions described in § 2, we calculate the distribution of the CO column density. We have found that the CO column density is nearly the same at $R \lesssim 250$ AU and is lower by less than an order of magnitude at $R \gtrsim 250$ AU, compared with those in Figures 4, 6, and 8 except for the case of $S = 0.3$ at $t = 10^6$ yr. In this case, the CO column density is decreased by photodissociation by many orders of magnitude at $R \gtrsim 250$ AU because CO molecules are almost totally adsorbed onto grains in the region shielded from the UV radiation. Because the self-shielding has been neglected, the above study gives an upper limit to the effect of the photodissociation. Therefore, we need not modify much the depletion factors listed in Table 4 with a possible exception of the case of $S = 0.3$ and $t = 1 \times 10^6$ yr.

5.2. *Nonthermal Desorption*

Although we have taken into account the effect of thermal desorption of molecules from dust grains, some nonthermal desorption processes may work in the interstellar medium and in the circumstellar disks. Some studies have been made on the molecular abundance in molecular clouds, taking into account the gas adsorption onto grain surfaces. In cool molecular clouds with temperature $T \sim 10$ K, which is lower than the critical temperature $T_{\rm crit}$ of CO, CO molecules are adsorbed to grains on a timescale $5 \times 10^6 (10^4 \text{ cm}^{-3}/n_{\rm H})(0.3/S)$ yr as can be seen from equation (9). Nevertheless, many kinds of gas molecules are detected in clouds by radio observations: the CO molecule especially is very abundant [$n({\rm CO})/n_{\rm H} \sim 10^{-4}$] in molecular clouds. To resolve this discrepancy, many nonthermal desorption mechanisms have been proposed: heating of dust by cosmic rays and X-rays (Léger, Jura, & Omont 1985), photoevaporation (d'Hendecourt et al. 1985; Hartquist & Williams 1990), and heating of dust by the energy released in exothermic reactions on grain surfaces (d'Hendecourt et al. 1982, 1985).

We shall check whether or not these mechanisms work effectively in the circumstellar disks. Dust in molecular clouds is heated impulsively by interstellar X-rays and cosmic rays. Léger et al. (1985) investigated the desorption due to whole grain heating by X-rays and by cosmic rays and due to spot heating by cosmic rays. They found that the whole grain heating by X-rays is efficient for grains of radius 2.0–4.0×10^{-6} cm and that the desorption rate amounts to 10^2–10^3 molecules cm^{-2} s^{-1} for these grains. They also found that the whole grain heating by cosmic rays is efficient for grains smaller than 2.0×10^{-5} cm by radius and that the desorption rate is several times 10^2 molecules cm^{-2} s^{-1} for these grains. The desorption rate by cosmic-ray spot heating found by them is about 70 molecules cm^{-2} s^{-1} irrespective of the grain size. Although these processes may be effective in molecular clouds in which the gas density is low, they are not so efficient as to keep most molecules in the gas phase in circumstellar disks in which the adsorption rate is very high because of high density.

Let us consider the effect of the X-rays from the central star. The X-ray flux from a central T Tauri star at $R \approx 100$ AU is about 5×10^4 times higher than the flux in the interstellar space (Bertout 1989; Montmerle et al. 1993). With such strong X-ray flux, the desorption rate would be higher than the adsorption rate of CO molecules in the surface layer of the disk containing about 0.71% (at $R = 300$ AU) to 2.4% (at $R = 800$ AU) of the column density if a sufficient amount of grains are small enough to be heated as a whole.

The ultraviolet photons can desorb molecules, since the photon energy is higher than the adsorption energy of a molecule on the grain. However, the efficiency, or the number of molecules desorbed by a single photon, remains uncertain. Hartquist & Williams (1990) adopt a value of 0.1, while d'Hendecourt et al. (1985 and references therein) insist

that the efficiency is as low as 10^{-6}. If the efficiency is as high as 0.1, the desorption rate is higher than the adsorption rate in the surface layer of the disk containing about 2.2% (at 300 AU) to 13% (at 800 AU) of the column density.

D'Hendecourt et al. (1982, 1985) proposed a mechanism called chemical explosion: if a grain is irradiated by ultraviolet radiation, many radicals are produced on the grain surface, and they would react explosively once the grain temperature gets higher than 27 K. The heat released by the exothermic reactions would be sufficient to evaporate the grain mantle. Léger et al. (1985) estimated the explosion rate in the case in which cosmic rays or X-rays would raise the grain temperature to trigger the explosion. As in the case of the impulsive heating cited above, efficient heating occurs by X-rays on the grains of radius $a \approx 2.0$–4.0×10^{-6} cm and by cosmic rays on the grains of $a \lesssim 2.0 \times 10^{-5}$ cm. Using the explosion rate obtained by them, we have found that the timescale of explosion by the X-rays from interstellar space is shorter than the adsorption timescale τ_{ads} in the surface layer containing about 2.5% (at $R \approx 300$ AU) to 35% (at $R \approx 800$ AU) of the column density. The X-rays from the central star have been found less effective. Similarly, the timescale of explosion by the cosmic rays is shorter than the adsorption timescale τ_{ads} in the surface layer containing about 0.3% (at $R \approx 300$ AU) to 9.5% (at $R \approx 800$ AU) of the column density.

More studies on the mechanisms of nonthermal desorption are needed for more quantitative discussion.

5.3. *Mixing of Matter*

There may be turbulence in the disk that can mix matter. An accretion flow may also appear in the disk and change the distribution of CO. We discuss here the effects of these on the depletion factor of CO in the disks. As shown in § 3.1, the CO molecules are chemically stable under the density and temperature of the circumstellar disks and in the timescale of $\lesssim 10^6$ yr, in which we are interested. It is the adsorption onto the grain surface that can affect efficiently the abundance of gas-phase CO molecules. Since the adsorption of CO molecules is strongly dependent on the temperature, transport of matter to the region of different temperature may greatly modify our results.

In the region of $R \gtrsim 100$ AU, the density n_H is lower than 2.0×10^9 cm^{-3} as seen from equation (4). At such densities, the magnetic field is coupled with the gas fairly well (Umebayashi & Nakano 1988; Nakano 1991). Therefore, this part of the disk suffers from the shear instability that can excite turbulence (Balbus & Hawley 1991; Hawley & Balbus 1991). Turbulence may transport the matter in the region of $T > T_{crit}$ containing much CO outward and as a result may change the distribution of the depletion factor of CO.

The turbulence velocity v_{turb} is significantly smaller than the sound velocity

$$C_s = \left(\frac{kT}{\mu m_H}\right)^{1/2} \approx 2.6 \times 10^4 \left(\frac{R}{200\ \mathrm{AU}}\right)^{-1/4} \mathrm{cm\ s^{-1}}, \quad (15)$$

and the mixing length, or the size of the largest eddies, l_{turb}, must be considerably smaller than the scale height of the disk, H, which is given from equation (4) by

$$\frac{H}{R} = \left(\frac{2kTR}{GM_* \mu m_H}\right)^{1/2} \approx 0.18 \left(\frac{R}{200\ \mathrm{AU}}\right)^{1/4}. \quad (16)$$

The matter is transported by the turbulence for a radial distance $\Delta R (\gg l_{turb})$ in a time

$$t_{mix}^{(R)} \approx \frac{(\Delta R)^2}{l_{turb} v_{turb}} \approx 2.0 \times 10^6 \left(\frac{\Delta R}{200\ \mathrm{AU}}\right)^2 \left(\frac{200\ \mathrm{AU}}{R}\right) \times \left(\frac{0.1H}{l_{turb}}\right)\left(\frac{0.1C_s}{v_{turb}}\right) \mathrm{yr}. \quad (17)$$

Thus it takes 2×10^6 yr or more to transport the matter in the region of $T > T_{crit}$ to the main part of the region in which CO is highly depleted. Because most of CO molecules are adsorbed to grains in this time, the turbulent mixing in the radial direction can hardly change the distribution of the CO depletion.

The turbulence can also mix the matter in the vertical (Z) direction. Desorption of CO may occur in the matter brought up to the high-Z region by the action of UV radiation, X-rays, and cosmic rays and may affect the depletion factor significantly. The mixing time of matter in the Z-direction can be given by

$$t_{mix}^{(Z)} \approx \frac{H^2}{l_{turb} v_{turb}} \approx 1.8 \times 10^5 \left(\frac{R}{400\ \mathrm{AU}}\right)^{3/2} \left(\frac{0.1H}{l_{turb}}\right)\left(\frac{0.1C_s}{v_{turb}}\right) \mathrm{yr}. \quad (18)$$

Thus, it seems rather difficult to keep the CO abundance considerably higher than that at $t \approx 10^5$ yr in our model.

5.4. *Coalescence and Sedimentation of Dust Grains*

As equation (9) shows, the timescale of adsorption of gaseous molecules onto grains is inversely proportional to the sum of the geometrical cross sections, or the total surface area, of grains contained in a unit volume. This quantity may decrease by coalescence of grains and also by their sedimentation. We shall discuss here whether or not these processes are efficient in decreasing the adsorption rate.

In a quiescent disk, the dust grain at a position (R, Z) sinks toward the equatorial plane on a timescale

$$t_{sed}(R, Z) \approx \frac{\rho_g(R, Z) H t_K}{2\pi a \rho_d} \approx 5.4 \times 10^6 \left(\frac{1.0 \times 10^{-5}\ \mathrm{cm}}{a}\right) \times \left(\frac{3\ \mathrm{g\ cm^{-3}}}{\rho_d}\right)\left[\frac{n_H(R, Z)}{n_H(R, Z=0)}\right] \mathrm{yr}, \quad (19)$$

where a and ρ_d are the radius and the density, respectively, of the grain; ρ_g is the gas density; and t_K is the Keplerian orbital period (Nakagawa, Nakazawa, & Hayashi 1981). The last expression of this equation is for the disk with the surface density distribution given by equation (1) and does not depend on R near the equatorial plane $|Z| \ll H$. As long as the grain radius is kept at $\sim 1.0 \times 10^{-5}$ cm, the sedimentation time is too long to prevent the adsorption of molecules except at $|Z| \gg H$.

The grains may grow by sticking when they collide with each other. This may accelerate their sedimentation and also may decrease the total surface area of grains. Nakagawa et al. (1981) considered two processes that lead to the collision of grains. One is their thermal Brownian motion. The other is that because larger grains sink faster as equation (19) shows, they collide with smaller grains sinking more slowly. In the outer regions of the disk, e.g., $R \gtrsim 100$ AU, the latter occurs much more frequently than the

former. According to Nakagawa et al. (1981), the collision time by this process at height Z is given by

$$t_{\rm col} \approx \frac{2}{3\pi\zeta}\frac{H}{Z}t_{\rm K} \approx 9\times 10^4\left(\frac{6.24\times 10^{-3}}{\zeta}\right) \times\left(\frac{H}{Z}\right)\left(\frac{R}{200\ {\rm AU}}\right)^{3/2}\ {\rm yr}\ , \quad (20)$$

where ζ is the fraction of solid by mass. Because the sticking probability of grains must be significantly smaller than unity, the collisional growth time must be considerably longer than 10^5 yr at $R \gtrsim 200$ AU.

Thus, it takes more than 10^5 yr to decrease the total surface area of grains per unit volume by coalescence and/or sedimentation in the major part of the disk at $R \gtrsim 200$ AU, which is much longer than $\tau_{\rm ads}$. Therefore, coalescence and sedimentation have little effect on preventing the adsorption of molecules in this part of the disk.

5.5. *Uncertainties in the Disk Temperature*

The temperature distribution given by equation (2) has been obtained by assuming that the disk is heated by the radiation from the central star. There must be some other heating sources such as cosmic rays and disk viscosity. We have found that there is a critical distance from the star, $R_{\rm crit}$, outside which CO is highly depleted at $t \sim 10^5$ yr, and at which the temperature takes the critical temperature $T_{\rm crit} \approx 20$ K for CO adsorption. At the outer edge of the disk $R \approx 800$ AU, equation (2) gives $T \approx 10$ K. With the ordinary cosmic-ray intensity (Spitzer & Tomasko 1968), the gas is heated only up to several kelvins. Because the disk masses we have adopted are rather small, we cannot expect a high accretion rate in the disk. We can easily confirm that by viscous heating even with an accretion rate $\dot{M} = 10^{-6}\ M_\odot\ {\rm yr}^{-1}$, the disk at $R \gtrsim 200$ AU is heated at most up to 10 K with the surface density given by equation (1). Thus, $R_{\rm crit}$ is hardly affected, and the depletion at $R \approx 800$ AU is not much affected by the other heating processes.

5.6. *Nonsteadiness of Disks*

Although we have assumed that the disk is in a steady state, or the temperature and density do not change with time, T Tauri stars show various variabilities. However, the temperature of the disk is not sensitive to the stellar luminosity as seen from equation (2). Outbursts such as FU Orionis phenomena suggest that episodic accretion occurs around T Tauri stars. However, such episodic phenomena are suggested to occur only in the region not very far from the stellar surface (Bell & Lin 1994). Accretion must be nearly steady in the outer part of the disk. Thus, the outer part of the disk must be kept almost in a steady state.

6. SUMMARY

We have investigated the evolution of the molecular abundance in the gaseous disks around young stars, taking into account the adsorption of gas molecules onto grain surfaces as well as the gas-phase reactions. In this paper, we have shown only the results on the abundance of CO in the gas phase.

There is a critical temperature $T_{\rm crit}$ for the adsorption of CO, which is about 20 K almost independent of the density and is significantly lower than those of the other molecules except for H_2. When the temperature is lower than $T_{\rm crit}$, CO molecules are adsorbed to grains efficiently. Even if the temperature is somewhat higher than the critical value for CO molecules, the abundance of CO would decrease ultimately because by gas-phase reactions CO may be transformed into other molecules that can be adsorbed much more easily. Because the timescale of adsorption, $\tau_{\rm ads}$, is inversely proportional to the density, the adsorption proceeds more efficiently in the region of higher density.

We have followed numerically the evolution of molecular abundance in some model disks. There is a critical distance from the central star, $R_{\rm crit}$, at which the temperature is equal to the critical temperature $T_{\rm crit}$ for the adsorption of CO. At $R > R_{\rm crit}$, CO molecules are depleted from the gas phase mainly because of the adsorption on a timescale $\tau_{\rm ads}$, while at $R < R_{\rm crit}$, the depletion is not so significant. For the minimum-mass solar nebula extended to the region of radius $R \approx 800$ AU, CO molecules at $R > R_{\rm crit} \approx 200$ AU are depleted by a few orders of magnitude in 10^5–10^6 yr. This is consistent with the recent observations of gaseous disks around some T Tauri stars.

We would like to thank T. Yamamoto, M. Hayashi, Y. Nakagawa, and S. Sasaki for helpful discussions and our referee for many suggestions to improve the paper. The calculations were performed partly at Astronomical Data Analysis Center of National Astronomical Observatory, Japan. This work is supported by Grant-in-Aid for Cooperative Research (C) from the Ministry of Education, Science, Sports, and Culture, Japan (07640363).

REFERENCES

Adams, F. C., Lada, C. J., & Shu, F. H. 1987, ApJ, 312, 788
Allen, M., & Robinson, G. W. 1977, ApJ, 212, 396
Appenzeller, I., Jankovics, I., & Östreicher, R. 1984, A&A, 141, 108
Avgul, N. N., & Kiselev, A. V. 1970, in Chemistry and Physics of Carbon, Vol. 6, ed. P. L. Walker (New York: Marcel Dekker), 1
Balbus, S. A., & Hawley, J. F. 1991, ApJ, 376, 214
Bally, J., & Langer, W. D. 1982, ApJ, 255, 143
Beckwith, S. V. W., Sargent, A. I., Chini, R. S., & Güsten, R. 1990, AJ, 99, 924
Bell, K. R., & Lin, D. N. C. 1994, ApJ, 427, 987
Bergin, E. A., Langer, W. D., & Goldsmith, P. F. 1995, ApJ, 441, 222
Bertout, C. 1989, ARA&A, 27, 351
Cameron, A. G. W. 1985, in Protostars and Planets II, ed. D. C. Black & M. S. Matthews (Tucson: Univ. of Arizona Press), 1073
d'Hendecourt, L. B., Allamandola, L. J., Baas, F., & Greenberg, J. M. 1982, A&A, 109, L12
d'Hendecourt, L. B., Allamandola, L. J., & Greenberg, J. M. 1985, A&A, 152, 130
Duley, W. W., & Williams, D. A. 1984, Interstellar Chemistry (New York: Academic)
Dutrey, A., Guilloteau, S., & Simon, M. 1994, A&A, 286, 149
Guilloteau, S., & Dutrey, A. 1994, A&A, 291, L23
Handa, T., et al. 1995, ApJ, 449, 894
Hartquist, T. W., & Williams, D. A. 1990, MNRAS, 247, 343
Hasegawa, T. I., & Herbst, E. 1993, MNRAS, 261, 83
Hawkins, I., Craig, N., & Meyer, D. M. 1993, ApJ, 407, 185
Hawley, J. F., & Balbus, S. A. 1991, ApJ, 376, 223
Hayashi, C. 1981, Prog. Theor. Phys. Suppl., 70, 35
Hayashi, C., Nakazawa, K., & Nakagawa, Y. 1985, in Protostars and Planets II, ed. D. C. Black & M. S. Matthews (Tucson: Univ. of Arizona Press), 1100
Herbig, G. H., & Goodrich, R. W. 1986, ApJ, 309, 294
Herbst, E. 1993, in Dust and Chemistry in Astronomy, ed. T. J. Millar & D. A. Williams (Bristol: IOP), 183
Imhoff, C. L., & Appenzeller, I. 1987, in Scientific Accomplishments of the *IUE*, ed. Y. Kondo (Dordrecht: Reidel), 295
Irvine, W. M., Goldsmith, P. F., & Hjalmarson, Å. 1987, in Interstellar Processes, ed. D. J. Hollenbach & H. A. Thronson, Jr. (Dordrecht: Reidel), 561
Kawabe, R., Ishiguro, M., Omodaka, T., Kitamura, Y., & Miyama, S. M. 1993, ApJ, 404, L63
Kenyon, S. J., & Hartmann, L. 1987, ApJ, 323, 714

Kusaka, T., Nakano, T., & Hayashi, C. 1970, Prog. Theor. Phys., 44, 1580
Langer, W. D., & Penzias, A. A. 1993, ApJ, 408, 539
Léger, A., Jura, M., & Omont, A. 1985, A&A, 144, 147
Mathis, J. S., Rumpl, W., & Nordsieck, K. H. 1977, ApJ, 217, 425
Mitchell, G. F., & Maillard, J.-P. 1993, ApJ, 404, L79
Montmerle, T., Feigelson, E. D., Bouvier, J., & André, P. 1993, in Protostars and Planets III, ed. E. H. Levy & J. I. Lunine (Tucson: Univ. of Arizona Press), 689
Morton, D. C. 1974, ApJ, 193, L35
Nakagawa, Y., Nakazawa, K., & Hayashi, C. 1981, Icarus, 45, 517
Nakano, T. 1991, Mem. Soc. Astron. Italiana, 62, 841
Ohashi, N., Kawabe, R., Hayashi, M., & Ishiguro, M. 1991, AJ, 102, 2054
Pollack, J. B., McKay, C. P., & Christofferson, B. M. 1985, Icarus, 64, 471
Prasad, S. S., & Huntress, W. T., Jr. 1980, ApJS, 43, 1
Prinn, R. G. 1993, in Protostars and Planets III, ed. E. H. Levy & J. I. Lunine (Tucson: Univ. of Arizona Press), 1005
Rucinski, S. M. 1985, AJ, 90, 2321
Saito, M., Kawabe, R., Ishiguru, M., Miyama, S. M., Hayashi, M., Handa, T., Kitamura, Y., & Omodaka, T. 1995, ApJ, 453, 384
Sandford, S. A., & Allamandola, L. J. 1988, Icarus, 76, 201
———. 1990, Icarus, 87, 188
Simon, M., & Guilloteau, S. 1992, ApJ, 397, L47
Skrutskie, M. F., et al. 1993, ApJ, 409, 422
Spitzer, L., Jr., & Tomasko, M. G. 1968, ApJ, 152, 971
Strom, K. M., Strom, S. E., Edwards, S., Cabrit, S., & Skrutskie, M. F. 1989, AJ, 97, 1451
Tielens, A. G. G. M., & Allamandola, L. J. 1987, in Interstellar Processes, ed. D. J. Hollenbach & H. A. Thronson, Jr. (Dordrecht: Reidel), 397
Umebayashi, T., & Nakano, T. 1988, Prog. Theor. Phys. Suppl., 96, 151
———. 1990, MNRAS, 243, 103
van Dishoeck, E. F., Blake, G. A., Draine, B. T., & Lunine, J. I. 1993, in Protostars and Planets III, ed. E. H. Levy & J. I. Lunine (Tucson: Univ. of Arizona Press), 163
Willacy, K., & Williams, D. A. 1993, MNRAS, 260, 635
Williams, D. A. 1993, in Dust and Chemistry in Astronomy, ed. T. J. Millar & D. A. Williams (Bristol: IOP), 143